Imaging study of vibrational predissociation of the HCl–acetylene dimer: pair-correlated distributions

Guosheng Li, Jessica Parr, Igor Fedorov and Hanna Reisler*

Received 1st March 2006, Accepted 27th March 2006
First published as an Advance Article on the web 13th April 2006
DOI: 10.1039/b603107b

The state-to-state predissociation dynamics of the HCl–acetylene dimer were studied following excitation in the asymmetric C–H (asym-CH) stretch and the HCl stretch. Velocity map imaging (VMI) and resonance enhanced multiphoton ionization (REMPI) were used to determine pair-correlated product energy distributions. Different vibrational predissociation mechanisms were observed for the two excited vibrational levels. Following excitation in the of the asym-CH stretch fundamental, HCl fragments in $v = 0$ and $j = 4$–7 were observed and no HCl in $v = 1$ was detected. The fragments' center-of-mass (c.m.) translational energy distributions were derived from images of HCl ($j = 4$–7), and were converted to rotational state distributions of the acetylene co-fragment by assuming that acetylene is generated with one quantum of C–C stretch (ν_2) excitation. The acetylene pair-correlated rotational state distributions agree with the predictions of the statistical phase space theory, restricted to acetylene fragments in $1\nu_2$. It is concluded that the predissociation mechanism is dominated by the initial coupling of the asym-CH vibration to a combination of C–C stretch and bending modes in the acetylene moiety. Vibrational energy redistribution (IVR) between acetylene bending and the intermolecular dimer modes leads to predissociation that preserves the C–C stretch excitation in the acetylene product while distributing the rest of the available energy statistically. The predissociation mechanism following excitation in the Q band of the dimer's HCl stretch fundamental was quite different. HCl ($v = 0$) rotational states up to $j = 8$ were observed. The rovibrational state distributions in the acetylene co-fragment derived from HCl ($j = 6$–8) images were non-statistical with one or two quanta in acetylene bending vibrational excitation. From the observation that all the HCl(j) translational energy distributions were similar, it is proposed that there exists a constraint on conversion of linear to angular momentum during predissociation. A dimer dissociation energy of $D_0 = 700 \pm 10$ cm^{-1} was derived.

I. Introduction

The hydrogen bond has been accepted as an important intermolecular binding force between a proton donor and acceptor, since the chapter, ''The Hydrogen Bond'' appeared in Pauling's 1939 book.[1] In the broadest definition, a proton acceptor can be an electron lone-pair or the polarizable electrons of a π bond. Understanding the nature of hydrogen bonding in environments ranging from the condensed to the gas phase,[2,3] including the structural organization of biomolecules,[4] has been a longstanding goal of chemical physics.[5–7] Due to their weak bond dissociation energies relative to covalent or ionic bonds, hydrogen bonds can be switched on or off within the range of thermal fluctuations at temperatures typical of living systems.[4] From a reaction dynamics point of view, studying hydrogen bonded complexes has revealed nonstatistical predissociation behavior, which is often mode dependent.[2,6,8] The goal of this work is to examine in detail vibrational energy redistribution (IVR) during predissociation, *i.e.* energy transfer through intermolecular and intramolecular coupling, and the existence of vibrational adiabaticity.[2,8,9]

In this study, velocity–map ion imaging (VMI) was combined with resonantly enhanced multiphoton ionization (REMPI) to obtain pair-correlated photofragment energy distributions from the vibrational predissociation of the HCl–acetylene dimer. These experiments require high resolution, because for each HCl rotational level there can be many correlated acetylene levels that have small energy gaps. The main advantage of the imaging technique is its ability to select (by REMPI) a specific rotational state of the HCl fragment and determine the translational energy distribution associated with it at a resolution that reveals the rotational distribution in the acetylene co-fragment. In addition, by using VMI the dissociation energy of the HCl–acetylene dimer can be determined accurately.

Information on the structure and spectroscopy of the HCl–acetylene dimer is known from microwave and infrared (IR) spectroscopy in the gas phase and Fourier transform infrared (FTIR) spectroscopy in matrix-isolation studies.[10–15] The geometry is ''T-shaped'' with the hydrogen bond forming between the hydrogen of HCl and the center of the distribution of π electrons of acetylene. Dayton *et al.* reported the first

Department of Chemistry, University of Southern California, Los Angeles, CA 90089-0482, USA. E-mail: reisler@usc.edu

high-resolution IR spectrum for the asymmetric C–H (asym-CH) stretch mode of the dimer.[14] By simulating the absorption spectrum of the dimer as a *b*-type transition, the band origin of the asym-CH stretch fundamental was determined at 3278.08 cm^{-1}, approximately 11 cm^{-1} red shifted from the band origin of the acetylene monomer. The high-resolution IR spectrum of the dimer's HCl stretch mode was measured by Carcabal *et al.*[15] It is red shifted by 79 cm^{-1} from the monomer origin—a much larger shift than that observed for the asym-CH stretch. The smaller red shift in the asym-CH stretch mode is attributed to its relatively small coupling to the hydrogen bond, in contrast to the HCl stretch motion, which is in the vicinity of the hydrogen bond. The linewidths observed in the high-resolution IR spectra range from 192 to 1037 MHz (depending on the rotational band) for the asym-CH stretch mode[14] and are 173 MHz for the HCl stretch mode.[15]

The vibrational predissociation of the dimer following asym-CH stretch excitation has previously been examined by two experimental groups.[14,16,17] They disagreed on the dimer's bond dissociation energy and the formation of HCl ($v = 1$) products. Oudejans and Miller (OM) concluded that HCl is produced only in $v = 0$, with acetylene co-fragments having one quantum of C–C stretch excitation (ν_2),[17] whereas Rudich and Naaman reported the observation of HCl in $v = 1$.[16]

In the present work, we report on the state-to-state reaction dynamics of the vibrational predissociation of the HCl–acetylene dimer following excitation in both asym-CH stretch and HCl stretch modes. The dimer's bond dissociation energy was determined at $D_0 = 700 \pm 10$ cm^{-1} and the pair-correlated distributions of specific HCl(*j*) states were analyzed. We conclude that different vibrational predissociation mechanisms take place following asym-CH and HCl stretch excitations and propose that the coupling between the intermolecular and intramolecular modes that governs vibrational to vibrational (V–V) and vibrational to transnational (V–T) energy transfer is sensitive to the location of the initial vibrational mode excited in the dimer. We confirm that the dynamics following asym-CH stretch excitation is governed by V–V transfer to the C–C acetylene stretch. In contrast, energy transfer following HCl stretch excitation resembles that in a hard sphere collision, and we suggest that constraints on linear to angular momentum transfer, as described in the hard ellipsoid model of McCaffery,[18] can explain qualitatively the experimental results of this work.

II. Experiment

Vibrational predissociation of the HCl–acetylene dimer formed in a pulsed supersonic molecular beam was studied following pulsed IR laser excitation. Rotationally excited HCl fragments were ionized by 2 + 1 REMPI and detected by time-of-flight (TOF) mass spectroscopy and VMI.[19]

HCl–acetylene dimers were formed in a pulsed nozzle (piezoelectric, 0.5 mm orifice) by supersonic expansion of a mixture of 5% HCl (Matheson Trigas, 99.999%) and 10% acetylene (Matheson Trigas) in He (99.9999%) at 2 atm stagnation pressure. Acetylene was purified by trap-to-trap distillation at the temperature of an ethanol/CO_2 slush bath to minimize acetone contamination. After supersonic expansion, the molecular beam was collimated by a skimmer (1.0 mm orifice, Beam Dynamics) before intersecting at right angles in the ion-acceleration lens assembly two-counter propagating and linearly polarized pulsed laser beams. The timing of the lasers' firings was carefully optimized to excite dimers in the early part of the molecular beam pulse, where their highest relative abundance was found. An estimate of the rotational temperature in the molecular beam was obtained at $T = 5$ K from the REMPI spectrum of the HCl monomer monitored through the $V\,(12) \leftarrow X(^1\Sigma^+)(0)$ transition near 236 nm.[20,21]

Pulsed IR radiation was generated from an OPO-OPA system (LaserVision, 0.4 cm^{-1}, 18–22 mJ at 2700–3400 cm^{-1}) pumped by a Nd:YAG laser (Continuum, PRII 8000). The frequency was calibrated by monitoring the asym-CH stretch vibration of methane in a photoacoustic cell.[22,23] Rotationally excited HCl fragments were detected by 2 + 1 REMPI using the *Q* branch of the $f(^3\Delta_2) \leftarrow X(^1\Sigma^+)$ transition at 243.81–243.90 nm as the intermediate.[21] The REMPI ultraviolet (UV) laser radiation was generated by frequency doubling the output of a dye laser system (Continuum, ND6000, Coumarin 480, 0.07 cm^{-1}) pumped by a Nd:YAG laser (Spectra Physics, GCR 230). The polarizations of the IR and UV laser beams were maintained parallel to the plane of the ion image, *i.e.* perpendicular to the TOF axis. The IR (2.5 mJ) and UV (0.07 mJ) laser beams were focused by lenses of 40.0 and 20.0 cm focal length, respectively. The time delay between the IR and UV lasers was fixed by a time delay generator (Stanford, DG535), which was controlled by a computer through a GPIB interface (National Instrument). The spectra were obtained by alternately taking an average under "IR on" and "IR off" conditions, where "IR on" indicates that the IR laser was fired 20 ns earlier than the UV laser and "IR off" indicates that the IR laser was fired 1.0 μs after the UV laser.

The VMI arrangement was described in detail elsewhere.[19,24,25] In brief, it consists of a four lens ion-acceleration assembly,[26] a 60 cm long drift-tube and a CCD camera (LA Vision, Imager) that monitors a phosphor screen coupled to a MCP ion detector (BURLE electro-optics Co.). This setup was operated in two modes: (i) TOF mass spectrometer for spectroscopy experiments and (ii) VMI for translational energy distributions. Due to the small translational energy of the fragments, the voltages applied to the ion-acceleration lens were reduced to expand the size of images for improved resolution. An event counting method was used to collect the raw two-dimensional (2-D) images,[27] and the 2-D images were converted to three-dimensional (3-D) velocity distributions using the basis set expansion (BASEX) method.[28] The resolution of the VMI experiment is $\Delta\nu \cong 30$ m s^{-1} and is determined primarily by parameters of the molecular beam expansion.

III. Results and analysis

1. HCl(*j*) photofragment yield spectra

We obtained IR spectra of the dimer in the range of the asym-CH stretch and HCl stretch fundamentals by monitoring HCl photofragments in selected rotational levels by REMPI while

Table 1 Spectroscopic constants for the HCl–acetylene dimer (all values are given in cm^{-1})

	Asym-CH stretch[a]	HCl stretch[b]
A''	1.20363 (30)	1.196 (4)
B''	0.08270 (20)	0.08275 (1)
C''	0.07696 (22)	0.07703 (1)
A'	1.19403 (37)	1.194 (1)
B'	0.08206 (24)	0.08394 (2)
C'	0.07726 (21)	0.07859 (2)
ν_0	3278.0784 (20)	2806.9172 (2)

[a] Ref. 17. [b] Ref. 15.

scanning the IR laser frequency. High-resolution IR absorption spectra have been investigated previously in this region,[16,17] and the derived molecular spectroscopic constants are summarized in Table 1.

HCl REMPI spectra obtained following excitation of the dimer's asym-CH stretch show that HCl in $\upsilon = 0$ was produced in rotational states up to $j = 7$, as shown in Fig. 1. Rotationally resolved IR spectra obtained by monitoring HCl photofragments in $j = 4$–7 are shown in Fig. 1a as insets. These spectra are in good agreement with simulations (*b*-type transition) calculated using the molecular constants given in Table 1 and an example is shown in Fig. 1b for HCl ($j = 7$) yield spectrum. Notice that the relative heights of the *K* bands in the IR photofragment yield spectra are not reproduced in the simulation. This is because the observed IR spectra are obtained by recording photofragment yields (action spectra) and their shapes depend on the fractional yield of the monitored HCl (*j*) fragment in exciting different *K* levels. For example, we observe that K_a ($1 \leftarrow 0$) increases in relative intensity when monitoring low *j* states of HCl.

When monitoring HCl in $j < 5$ enhanced absorption features appear to the red of the dimer's spectrum. These features are typical of larger complexes. For example, spectral features at <3270 cm^{-1} are similar to IR absorption features of large acetylene complexes that have been studied by high-resolution IR spectroscopy.[29] Although enhancements are observed for HCl $j = 3$ photofragments with "IR on", as shown in Fig. 1a, the IR spectrum was not rotationally resolved, indicating that most of the HCl ($j = 3$) photofragments are produced in the dissociation of larger complexes.

HCl REMPI spectra following HCl stretch excitation of the dimer are shown in Fig. 2. HCl(*j*) yield spectra were obtained for $j = 6$–8 where enhancements are significant. The yield spectra are in good agreement with *a*-type simulations of the HCl stretch of the dimer obtained by using the molecular constants given in Table 1. When monitoring HCl ($j = 3$–5), the IR spectra do not show the typical structures of the dimer even though enhancement is seen. This observation is similar to the case discussed above for the asym-CH stretch. Spectral contamination from larger complexes increases on the higher frequency side (>2810 cm^{-1}) as seen in Fig. 2a. This frequency range is close to IR absorptions of the HCl dimer[30,31] and trimer.[32]

Three experimental conditions allow observation of predissociation events predominantly from the HCl–acetylene dimer: (1) state selective pumping of the dimer in the asym-CH stretch or the HCl stretch mode, which helps eliminate predissociation of larger complexes; (2) enhancements in state-selective signals from specific HCl(*j*) photofragments; and (3) monitoring the early part of the pulsed molecular beam (30 μs time window in a 300 μs pulse width) to optimize the relative population of HCl–acetylene dimers.

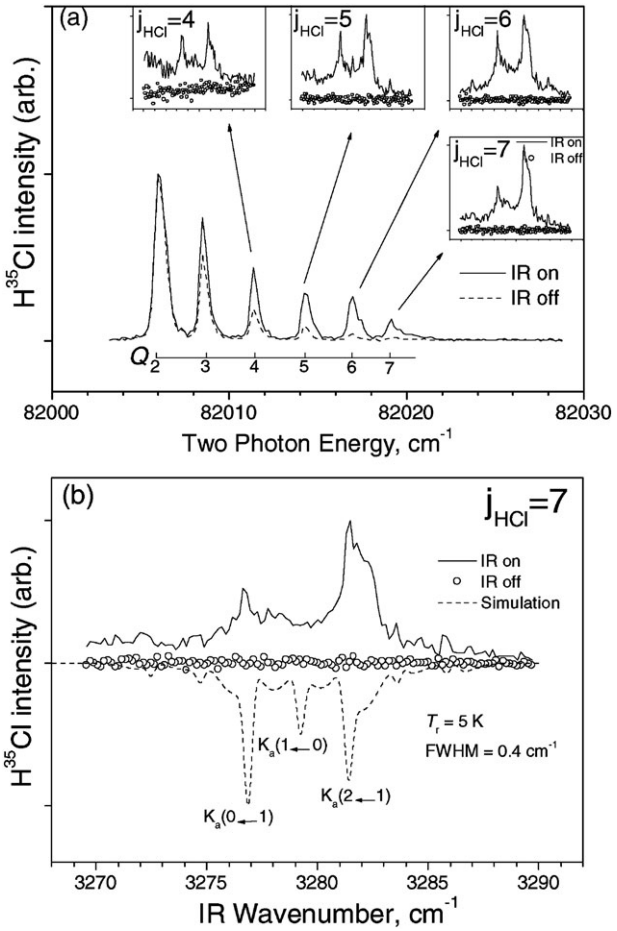

Fig. 1 (a) HCl photofragment 2 + 1 REMPI spectra obtained by exciting the $K_a = 2 \leftarrow 1$ transition of the asym-CH stretch of the HCl–acetylene dimer at 3281.4 cm^{-1} and scanning the UV laser through the *Q* branch of the $f(^3\Delta_2) \leftarrow X(^1\Sigma^+)$ transition of HCl with "IR on" (solid) and "IR off" (dotted), respectively. Transitions from $j = 0$ and 1 are not shown, because they are heavily perturbed. HCl ($j = 4$–7) photofragment yield spectra are shown as insets. (b) HCl ($j = 7$) fragment yield IR spectrum (solid) compared to a simulated spectrum (dotted) of a *b*-type transition calculated with molecular constants given in Table 1.

2. Rotational state distributions of HCl and acetylene fragments

The global rotational state distribution of HCl fragments was directly obtained from the 2 + 1 REMPI spectra of HCl ($\upsilon = 0$) shown in Fig. 1 and 2, after background subtraction. The relative HCl(*j*) populations obtained following asym-CH stretch and HCl stretch excitations are given in Table 2. Populations are presented only for those levels that show both significant enhancement and typical IR spectra of the HCl–acetylene dimer. No HCl in $\upsilon = 1$ was observed.

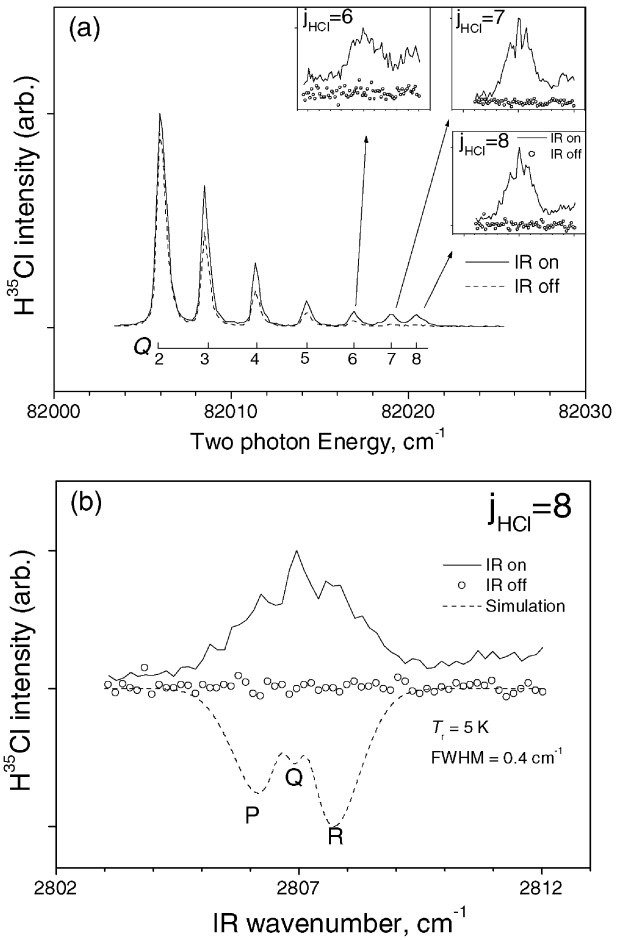

Fig. 2 (a) HCl photofragment 2 + 1 REMPI spectra obtained by exciting the Q branch of the HCl stretch of the HCl–acetylene dimer at 2806.9 cm^{-1} and scanning the UV laser through the Q branch of the $f(^3\Delta_2) \leftarrow X(^1\Sigma^+)$ transition of the HCl with "IR on" (solid) and "IR off" (dotted), respectively. HCl (j = 6–8) photofragment yield spectra are shown as insets. (b) HCl (j = 8) fragment yield IR spectrum (solid) compared to a simulated spectrum (dotted) of an a-type transition calculated with molecular constants given in Table 1.

Global rovibrational state distributions in the acetylene fragment were not measured, but pair-correlated distributions were derived from the HCl(j) images as described below. In assigning rovibrational states of the acetylene co-fragment, restrictions on rotational state populations imposed by nuclear spin statistics in the predissociation were taken into account. The correlation between the K_a level of the HCl–acetylene dimer and the j state of the acetylene co-fragment has been discussed by Miller and coworkers.[17,33] Briefly, for asym-CH stretch excitation, even (odd) K_a states of the dimer can produce odd (even) rotational states of acetylene fragments when the vibrational symmetry of the acetylene fragment is *gerade* (*ungerade*). The corresponding correlations for the dimer's HCl stretch excitation are: even (odd) K_a states of the dimer can produce even (odd) rotational states of the acetylene fragment when the vibrational symmetry of acetylene fragment is *gerade* (*ungerade*).

In our experiments, $K_a = 1 \leftarrow 0$, $0 \leftarrow 1$ and $2 \leftarrow 1$ transitions of the asym-CH stretch fundamental are resolved, as seen in Fig. 1b. The rotational states of the acetylene fragments produced following $K_a = 2 \leftarrow 1$ transitions will be distributed in even or odd rotational states depending on the vibrational mode of the acetylene fragment following the rules above. The situation for HCl stretch excitation is different: the monitored Q branch of the a-type band is very congested and the IR laser bandwidth is too large to resolve individual K_a transitions. Therefore, the acetylene's rotational states can be both even and odd rotational states. This is taken into account in the analyses presented below.

2(a). Pair-correlated acetylene state distributions following asym-CH strech excitation. 2-D cuts of reconstructed 3-D images of HCl($v = 0$, j = 4–7) photofragments produced following excitation of the asym-CH stretch ($K_a = 2 \leftarrow 1$) of the dimer are shown in Fig. 3. The corresponding center-of-mass (*c.m.*) translational energy distributions obtained by applying energy and momentum conservation are presented in Fig. 4. In our case, energy conservation is given by:

$$D_0(\text{dimer}) = h\nu + E_p(\text{dimer}) - E_j(\text{HCl}) - E_{v,i}(C_2H_2) - E_j(C_2H_2) - E_T \quad (1)$$

where $h\nu$ is the energy of the IR photolysis photon, E_j(HCl) is the rotational energy of the HCl(j) fragment, $E_{v,i}(C_2H_2)$ and $E_j(C_2H_2)$ are the vibrational and rotational energies of the acetylene co-fragment (with the subscript i indicating the different vibrational modes of the acetylene fragment) and E_T is the c.m. translational energy obtained from the measured translational energy of HCl(j). The internal energy of the dimer, E_p(dimer), is negligible in the molecular beam (T = 5 K). E_j(HCl) is calculated by using the rotational constants of HCl.[20,21]

Table 2 Rotational state distributions of HCl fragments from the vibrational predissociation of the HCl–acetylene dimers

HCl ($v = 0$)	Asym-CH stretch $K_a = 2 \leftarrow 1$ transition			HCl stretch Q band
	This work		Oudejans *et al.*[a]	This work
	Exp.	PST	Exp.	Exp.
$j \leq 3$	—	2.13	0.83	—
4	0.83 (0.10)[b]	0.97	0.44	—
5	0.90 (0.09)[b]	1.00	1.00	—
6	1.00 (0.10)[b]	0.75	0.50	0.63 (0.08)
7	0.60 (0.07)[b]	0.11	—	1.00 (0.11)
8	—		—	1.00 (0.11)

[a] Ref. 17. [b] Errors are shown in parentheses and reflect standard deviation.

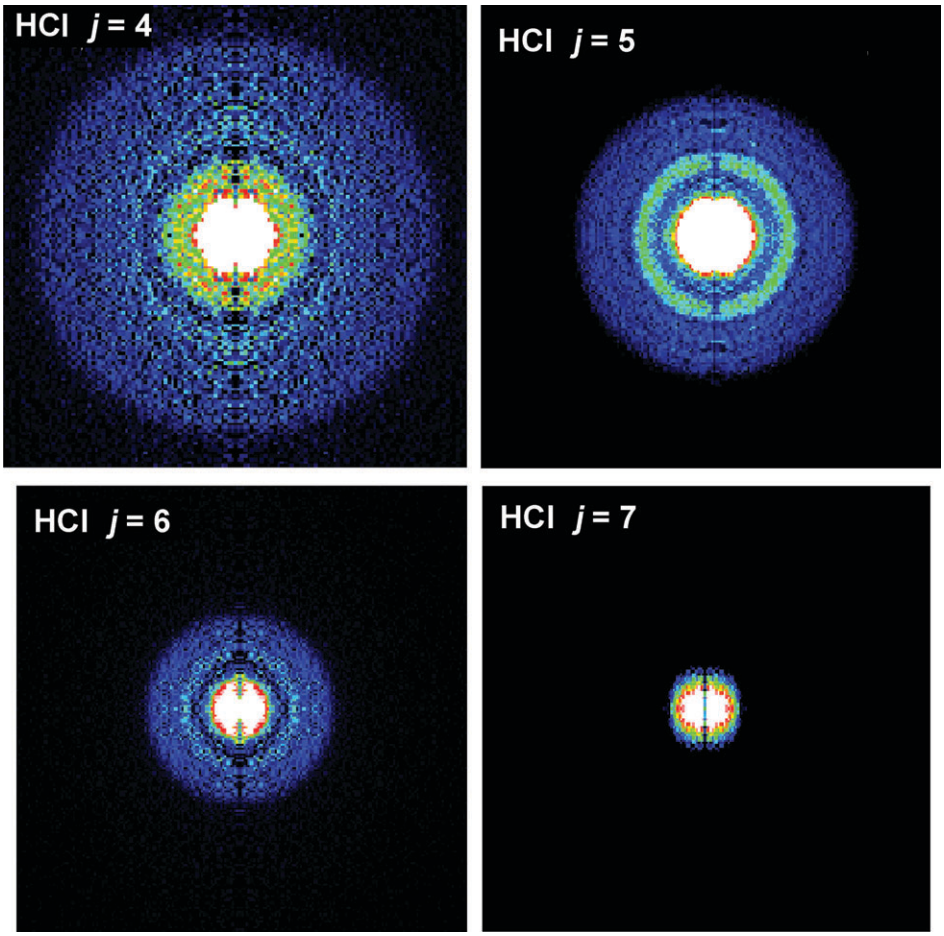

Fig. 3 2-D cuts in reconstructed images of HCl (j = 4–7) obtained by exciting the dimer in the $K_a = 2 \leftarrow 1$ transition of the asym-CH stretch at 3281.4 cm^{-1}. Note that the images become smaller as the monitored j state of HCl increases, reflecting the decrease in available energy.

To determine D_0(dimer) we need to know $E_{v,i}(C_2H_2)$ and $E_j(C_2H_2)$. By considering the energetically allowed combinations of acetylene rovibrational states, it should be possible to find a unique assignment that yields a single value of D_0 (dimer) for the dissociation channels terminating in HCl (j = 4–7). Previous studies have given indications how to narrow this search. Specifically, in predissociation of the HF–acetylene dimer, Miller and coworkers observed a propensity for excitation of one quantum of the ν_2 mode in the acetylene fragment in asym-CH stretch excitation.[33] They assumed the same propensity for the HCl–acetylene dimer system, which was not resolved in their experiments.[17] Making the same assumption in fitting our data, the fine structure in all the HCl(j) translational energy distributions is fit well by the rotational states of $C_2H_2(1\nu_2)$ when D_0(dimer) = 700 ± 10 cm^{-1}.

To obtain rotational state distributions, we fitted the translational energy distributions of each HCl(j) with a set of Gaussian functions, using a standard nonlinear least-squares routine, the Levenberg–Marquardt method.[34] The width of the Gaussian functions, which is related to the translational energy resolution, primarily depends on broadening by the molecular beam expansion conditions.

The nuclear spin selection rules described in the previous section are obeyed in the predissociation, at least for the high rotational levels, which are well resolved. This is demonstrated by the c.m. translation energy distributions shown in Fig. 5, which were obtained by exciting the dimer's asym-CH stretch *via* the $K_a = 2 \leftarrow 1$ and $K_a = 1 \leftarrow 0$ transitions. Examination of the low energy parts of the distributions shows that only odd acetylene rotational states are populated in the $K_a = 2 \leftarrow 1$ case and even ones in $K_a = 1 \leftarrow 0$. The low rotational levels of the acetylene, which have small energy separations and higher recoil energy, cannot be resolved in our experiment.

2(b). Pair-correlated acetylene state distributions following HCl stretch excitation. The c.m. translational energy distributions of HCl(j = 6–8) photofragments obtained following HCl stretch excitation are shown in Fig. 6. With the bond dissociation energy set at D_0(dimer) = 700 cm^{-1}, the ν_2 vibrational mode of the acetylene fragment is not energetically accessible. The allowed rovibrational states of acetylene are shown as short sticks in Fig. 6 and the dotted vertical lines indicate the translational energy thresholds for the energetically allowed vibrational levels of acetylene.

The high density of accessible rovibrational states of acetylene prevents us from obtaining a unique determination of the rovibrational state distributions. Nevertheless, it is possible to exclude several possibilities by careful examination of the translational energy distributions for different HCl(j) products. Let's examine first the possibility that two quanta

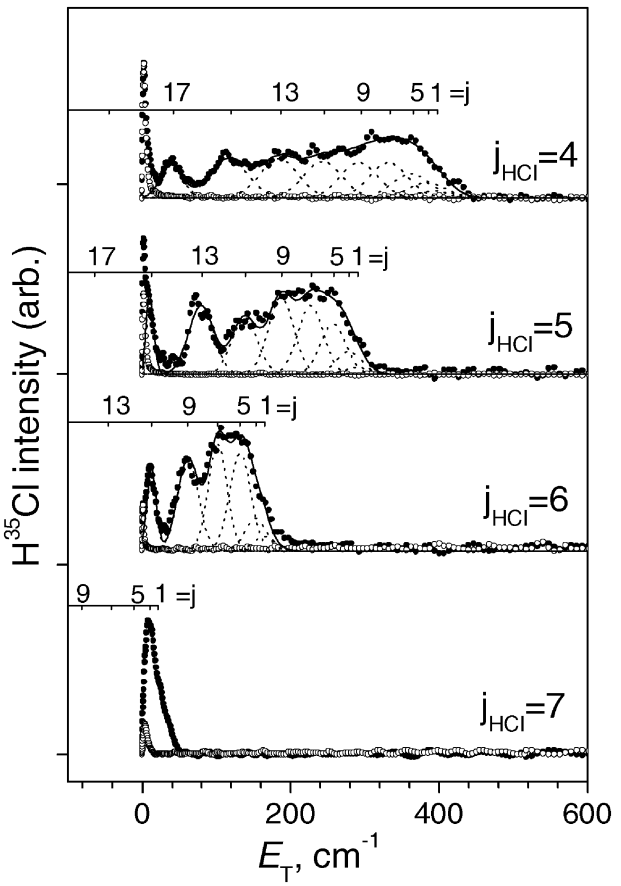

Fig. 4 Center-of-mass (c.m.) translational energy (E_T) distributions corresponding to images of HCl(j = 4–7) shown in Fig. 3. The odd j assignments correspond to rotational states of the acetylene co-fragment produced with one quantum in ν_2 (C–C stretch mode). See the text for details.

of bend, $2\nu_4$, $1\nu_4 + 1\nu_5$, or $2\nu_5$ (where ν_4 is the *cis*-bend and ν_5 is the *trans*-bend), are populated. By inspection of the translational energy distributions of HCl in j = 6 and 7 in Fig. 6, these combinations appear to provide a good fit if rotational excitation is added to each vibration. However, for HCl(j = 8) two quanta of bend alone are not sufficient to fit the data, because products with higher translational energies than allowed energetically are generated. The next possibility is an acetylene product with one quantum of bend excitation, *i.e.*, $1\nu_4$ or $1\nu_5$. In this case, the translational energy distributions can be matched, albeit with high rotational excitation in the acetylene fragment. Referring to energy conservation, there are two issues: (1) can highly rotationally excited acetylene fragments be produced; and (2) why HCl(j = 9) is not detected? If formation of highly rotationally excited product states is allowed, then HCl(j = 9) should also be observed, but it is not. Thus, product rotation appears to be restricted.

Production of acetylene in its ground vibrational state can be discounted. This channel should be accompanied by high rotational excitation of the acetylene co-fragment. The translational energy resolution of our imaging arrangement is sufficient to resolve such high levels, as demonstrated in Fig. 4 and 5, but they are not seen. Therefore, it is most likely

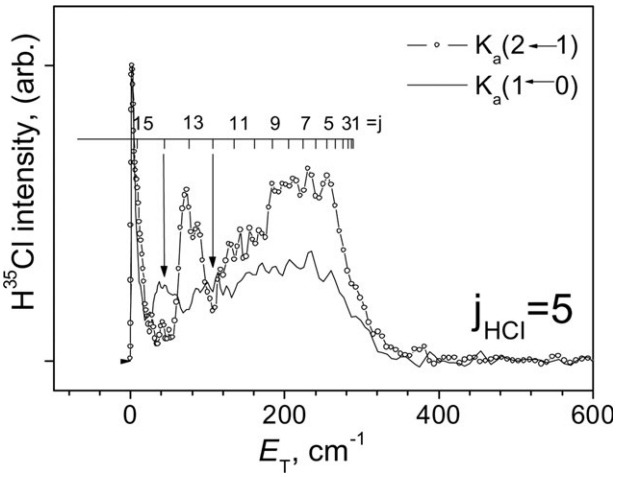

Fig. 5 Comparison of c.m. translational energy distributions obtained by pumping $K_a = 2 \leftarrow 1$ (solid line) and $K_a = 1 \leftarrow 0$ (circles with solid line) transitions of the asym-CH stretch, respectively, and monitoring HCl(j = 5). Odd and even j levels of the acetylene co-fragment are observed for $K_a = 2 \leftarrow 1$ and $K_a = 1 \leftarrow 0$ transitions, respectively. See the text for details.

that acetylene fragments are produced predominantly with one or two quanta of bending vibrational excitation.

IV. Discussion

1. Comparison with previous results

Predissociation of the HCl–acetylene dimer was studied before following excitation in the asym-CH stretch but not the HCl stretch. Rudich and Naaman concluded, based on their observation of HCl (v = 1) fragments, that the dissociation energy of the dimer was D_0 = 170–260 cm^{-1}.[16] However, no detailed IR photofragment yield spectra were presented to confirm that HCl(v = 1) fragments were produced from predissociation of the dimer and not from larger clusters. Later, OM used an optothermal detector to measure the photofragment angular distributions.[17] They did not observe HCl in v = 1 but found a propensity for populating one quantum of ν_2 in the acetylene fragment. The bond dissociation energy of $D_0 = 830 \pm 6$ cm^{-1} was obtained by fitting the angular distributions of the photofragments and assuming that acetylene co-fragments were populated only in low rotational states with an average rotational energy of 59 cm^{-1}.

The bond dissociation energy of $D_0 = 700 \pm 10$ cm^{-1} reported here, which differs by 130 cm^{-1} from the value of OM, was determined by a more direct method. Because the reported errors in the two values are small, the difference must derive from assumptions made in estimating D_0. In fact, the two values can be reconciled by shifting the HCl rotational distribution of OM by one quantum. In our work, the rotational state distribution in the HCl fragment was determined directly by REMPI, showing that levels up to j = 7 were populated with a maximum population in j = 6. The HCl(j) populations of ref. 17 were determined indirectly, by fitting the total product angular distribution, and OM concluded that levels up to j = 6 were populated, with a maximum in j = 5.

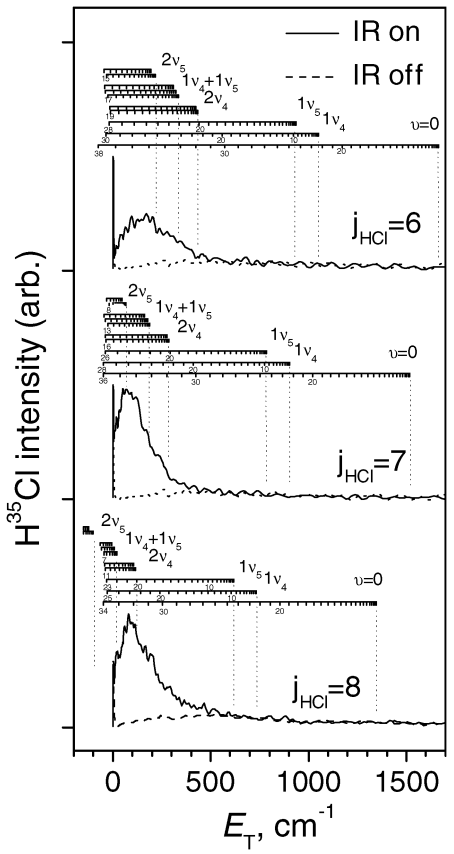

Fig. 6 C.m. translational energy distributions obtained by pumping the Q band of the HCl stretch of the dimer at 2806.9 cm^{-1} and recording images of HCl(j = 6–8). The dashed vertical lines indicate the translational energy thresholds for vibrational modes of the acetylene co-fragment assuming D_0 = 700 cm^{-1}. The sticks indicate the rotational states of each vibrational mode of the acetylene co-fragment; the numbers under the bars give the rotational state assignments. Both odd and even j can be populated, as explained in the text.

The second source of difference between the two results, which is smaller, derives from the rotational state distributions in the acetylene fragments. Our images show clearly that the rotational state distribution in the acetylene co-fragment depends on the HCl(j) level. In contrast, OM assumed similar distributions, all centered at low rotational levels. When we subtract the difference HCl(j = 7) − HCl(j = 6) = 146 cm^{-1} from the dissociation energy obtained by OM, a modified bond energy of D_0 = 684 ± 6 cm^{-1} is obtained, much closer to our value. The difference in the acetylene rotational state distributions accounts for the rest of the discrepancy between the two values.

The dimer's bond dissociation energy was also calculated by high level *ab initio* methods. A value of D_0 = 1.9 kcal mol^{-1} (665 cm^{-1}) was obtained by Pople *et al.* (MP4SDQ level on 6-31G* basis).[35] Later, D_0 = 2.00 kcal mol−1 (700 cm^{-1}) was obtained (with zero point energy correction to D_e) from MP2 perturbation and ACPF methods.[17,36] Recently, Carcabal *et al.* reported D_0 = 460 cm^{-1} by performing CCSD(T) calculations with cc-pVTZ basis set.[15] They also estimated values ranging from 291 to 608 cm^{-1} from analyzing their measured spectra. The bond dissociation energy obtained in this work is in good agreement with the majority of the *ab initio* calculations.

2. Comparison of rotational distributions with phase space theory (PST)

Because the pair-correlated rotational excitation in the acetylene co-fragment obtained following asym-CH stretch excitation decreases for higher HCl(j) levels, it is sensible to compare it to PST predictions. Rotational state distributions were computed for dissociation from the K_a = 2 dimer level, taking into account energy and angular momentum conservation.[6,37–39] Angular momentum conservation dictates that

$$\boldsymbol{J}(\text{dimer}) = \boldsymbol{j}(\text{HCl}) + \boldsymbol{j}(C_2H_2) + \boldsymbol{L} \qquad (2)$$

where J(dimer), j(HCl) and $j(C_2H_2)$ are the angular momenta of the HCl–acetylene dimer, HCl fragment and acetylene fragment, respectively, and L is the orbital angular momentum. In the calculations, J(dimer) was weighted according to a 5 K Boltzmann distribution.

We restricted the PST calculations by assuming, as in the fits shown in Fig. 4, that only the $1\nu_2$ level of the acetylene fragment is populated. The calculated and experimental rotational state distributions in acetylene fragments correlated with HCl j = 4–6 are shown in Fig. 7. Only odd rotational states of acetylene were considered for K_a = 2, as explained in the previous section.

The experimental and restricted PST calculations agree surprisingly well despite the fact that the vibrational distribution in acetylene is nonstatistical. It is well established that vibrational motions in the excited parent have different degrees of adiabaticity in evolution to products during unimolecular dissociation, *i.e.* vibrations become adiabatic at different points along the reaction coordinate.[2,6] In the case of the acetylene–HCl dimer, a model in which restricted IVR is combined with unimolecular decomposition can best explain the observed results. The C–C stretch in the acetylene fragment appears to be immune to further IVR and is isolated from the unimolecular reaction coordinate. The near resonance between the dimer's asym-CH stretch (∼3280 cm^{-1}) and a combination of C–C stretch (1974 cm^{-1}) and two quanta of acetylene bend (each ∼600 cm^{-1}) is the driving force for the initial V–V transfer within the acetylene moiety.[15] Following V–V transfer, it is reasonable to assume that breaking of the hydrogen bond proceeds by coupling of bending motions in acetylene to intermolecular vibrational modes in the dimer (calculated at 324, 260, 92 and 64 cm^{-1}).[15] These low frequency modes can couple effectively, giving rise to a statistical apportioning of energy among translational and rotational degrees of freedom of the products.

The relative rotational state populations of HCl fragments obtained in the experiment are given in Table 2, which also shows the values obtained by PST calculations. HCl(j) is populated up to the highest level predicted to be energetically allowed when acetylene products are being generated with one quantum of C–C stretch. The measured populations are not too different from PST predictions, except that the measured highest rotational levels appear to have larger populations than predicted by PST. This may reflect the well known

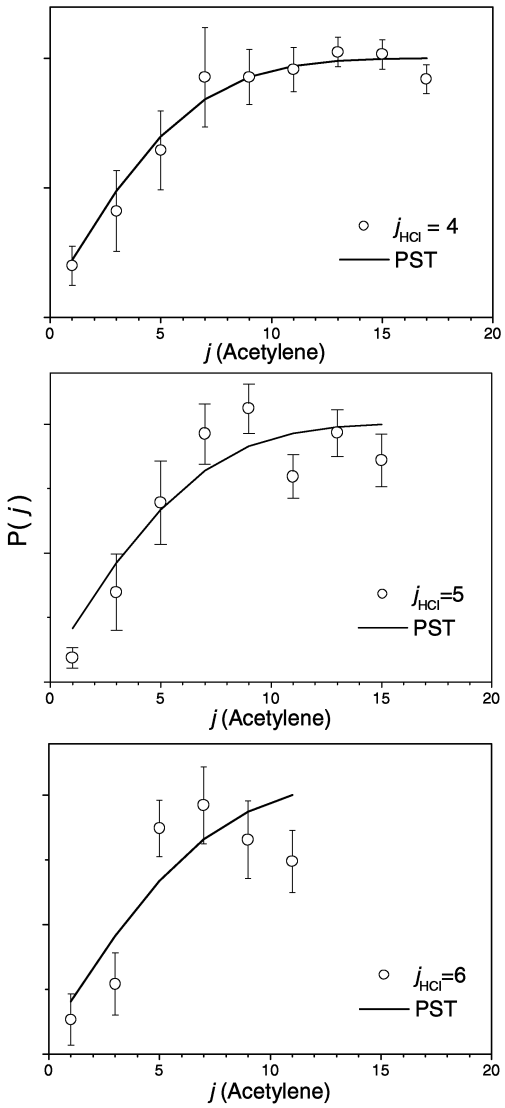

Fig. 7 Rotational state distributions of the acetylene fragment correlated with the HCl(j = 4–6) and obtained by exciting the K_a = 2 ← 1 band of the asym-CH stretch of the dimer. The circles show the experimental results and the solid line depicts the distribution obtained by PST.

propensity to minimize translational energy release in predissociation of complexes.[2,3]

In summary, the product state distributions obtained following asym-CH stretch excitation are dominated by the initial V–V transfer within the acetylene moiety of the dimer, which gives rise to C–C stretch and bend excitation and constitutes the rate determining step in this relatively slow predissociation. Subsequent efficient coupling between the acetylene bending modes and the intramolecular dimer modes leads to breaking of the hydrogen bond and results in largely statistical distributions of rotational and translational energies in the products.

3. Predissociation dynamics following HCl stretch excitation

As discussed above, the predissociation dynamics following HCl stretch and asym-CH stretch excitation are quite different. In contrast to the strong propensity for populating $1\nu_2$ in acetylene in the latter case, no propensity for a specific vibrational level is observed in the former. The acetylene fragments can be born with either zero, one, or two quanta of bending excitation and the ratio may depend on the co-fragment HCl(j) state. Oudejans *et al.*, who studied the predissociation of the HF–acetylene dimer following HF stretch excitation, also observed a broader vibrational distribution in the acetylene fragment than the one obtained in asym-CH stretch excitation.[33]

The maximum observed rotational level of HCl is j = 8, smaller than the highest level allowed energetically (j = 13 for acetylene in the ground vibrational state). This is in contrast to the case of asym-CH stretch excitation, where the highest allowed HCl level (j = 7) is produced along with $1\nu_2$ in acetylene. The most intriguing result is that the translational energy distributions for all the observed HCl(j) states are similar, as seen in Fig. 6. This suggests that the predissociation dynamics following asym-CH stretch and HCl stretch excitations differ in a way that is related to the different location of the excited dimer's vibrational level with respect to the motion of the hydrogen atom involved in the hydrogen bond. Whereas the asym-CH stretch and the C–C stretch vibrations are orthogonal to the hydrogen bond, the HCl stretch is parallel to it and therefore is coupled more efficiently to the dissociation coordinate, as attested to by the large frequency shift of the dimer's HCl stretch.

Several models can be considered in describing the predissociation dynamics. The well-known energy gap[40,41] or momentum gap law[42,43] models have been used widely to describe vibrational predissociation of van der Waals (vdW) complexes. According to this model, the dissociation rate is roughly proportional to the exponent of the negative term of the translational energy released for each product channel. Therefore, excitation of high internal degrees of freedom in the fragments would lead to low *c.m.* translational energy and an increase in the predissociation rate. The momentum gap law can qualitatively explain why a large fraction of the available energy goes to vibrational excitation of the acetylene fragment and rotational excitation of HCl and acetylene fragments. In addition, Ewing has proposed that the predissociation rate decreases in channels for which a large change in the number of quanta is required.[41] This disfavors products with high rotational excitation and may explain the propensity for bending excitation in the acetylene fragment that is accompanied by relatively low rotational excitation. It may also explain why HCl levels with j > 8 are not observed.

However, the momentum gap law does not explain why the *c.m.* translational energy distributions for all the measured HCl(j) states are similar. This observation suggests the existence of a kinematic constraint in the transformation of linear to angular momentum. Recently, several experimental and theoretical papers discussed the role of such a constraint in the predissociation of the vdW complexes.[18,44,45] McCaffery and coworkers represented the rotational distribution of fragments by considering the vibrational predissociation process as an internal collision within the vdW complex.[18,44,45] This approach treats the enhanced motion of the vibrational mode in the vdW complex as localized and approximates it as an

internal collision between an atom and a diatom. Forces act impulsively in the interaction region defined as a surface of a hard ellipsoid with dimensions related to the bond length of the diatom in the vdW molecule.[46,47] Linear-to-angular momentum transfer plays a central role in the kinematics under the constraint of energy conservation.

Application of this model to the HCl–acetylene dimer is complicated, but we can envision that when the HCl stretch is excited, the vibrational motion is mostly localized in the H atom due to its small mass and the linear acetylene can be approximated as a diatom. Consequently, the vibrational predissociation could be described qualitatively by the model proposed by McCaffery, in which the linear momentum of the H atom of HCl is converted to rotational angular momenta of both fragments, subject to kinematic constraints. In addition to the need to obtain a reasonable approximation for the equivalent hard ellipsoid potential for this larger complex, the model must account for the angular momenta of both HCl and acetylene. However, because it has treated successfully several cases in which similar constraints were observed, the model may be able to reproduce the limitation on the rotational excitation in HCl and the requirement that some energy remains in relative translation. A more quantitative explanation must await theoretical studies.

V. Summary

The predissociation dynamics of the HCl–acetylene dimer were studied using VMI at the pair correlated level. The dissociation energy of the dimer is found to be $D_0 = 700 \pm 10$ cm^{-1}. The predissociation mechanism depends on the initial vibrational level excited in the dimer. In the case of asym-CH stretch excitation, an accidental near-resonance exists between the dimer's asym-CH stretch fundamental and a combination of acetylene C–C stretch and two quanta of bend, which facilitates initial V–V transfer within the acetylene moiety. Subsequent coupling of the bends to the intermolecular modes of the dimer leads to unimolecular decomposition with near-statistical energy partitioning among the rotational and translational degrees of freedom of the products. The dimer's C–C stretch excitation evolves adiabatically to the acetylene product and no other vibrational levels in acetylene are excited. HCl is produced only in $v = 0$, with a rotational distribution that appears somewhat biased towards the highest rotational levels, in accordance with the momentum gap law.

A different mechanism is dominant in predissociation following excitation of the dimer's HCl stretch vibration, which is parallel to the dissociation coordinate. In this case, there is no preference for a specific vibrational level in the acetylene fragment. Rather, one or two quanta of *cis*- or *trans*-bend are predominantly excited and their relative populations vary with HCl(j) in a way that obeys the momentum gap law and minimizes the number of transferred quanta, as proposed by Ewing.[42] The observation of similar translational energy release in all the observed HCl(j) distributions suggests that the predissociation can be treated as a hard sphere collision, in which the transfer of linear to angular momentum is limited by a kinematic constraint. The hard ellipsoid model proposed by McCaffery may be able to describe quantitatively the energy partitioning in this case.[18]

Acknowledgements

This work is supported by the National Science Foundation. In interpreting our results, we benefited greatly from the pioneering work of Prof. R. E. Miller, who passed away last year.

References

1 L. Pauling, *The Nature of the Chemical Bond and the Structure of Molecules and Crystals; an Introduction to Modern Structural Chemistry*, Cornell University Press, New York, 1939.
2 L. Oudejans, R. E. Miller and W. L. Hase, *Faraday Discuss.*, 1995, **102**, 323–338.
3 M. I. Lester, *Adv. Chem. Phys.*, 1996, **96**, 51–102.
4 G. A. Jeffrey and W. Saenger, *Hydrogen Bonding in Biological Structures*, Springer-Verlag, Berlin Heidelberg, 1991.
5 R. Schinke, *Photodissociation Dynamics*, Cambridge University press, Cambridge, 1993.
6 T. Baer and W. L. Hase, *Unimolecular Reaction Dynamics*, Oxford University Press, New York, 1996.
7 M. N. R. Ashfold and J. E. Baggott, *Molecular Photodissociation Dynamics, Advances in Gas-Phase Photochemistry and Kinetics*, The Royal Society of Chemistry, London, 1987.
8 R. E. Miller, *Science*, 1988, **240**, 447–453.
9 J. B. Davey, M. E. Greenslade, M. D. Marshall, M. D. Wheeler and M. I. Lester, *J. Chem. Phys.*, 2004, **121**, 3009–3029.
10 A. C. Legon, P. D. Aldrich and W. H. Flygare, *J. Chem. Phys.*, 1981, **75**, 625–630.
11 P. D. Aldrich and E. J. Campbell, *Chem. Phys. Lett.*, 1982, **93**, 355–360.
12 L. Andrews, G. L. Johnson and B. J. Kelsall, *J. Phys. Chem.*, 1982, **86**, 3374–3380.
13 S. A. McDonald, G. L. Johnson, B. W. Keelan and L. Andrew, *J. Am. Chem. Soc.*, 1980, **102**, 2892–2896.
14 D. C. Dayton, P. A. Block and R. E. Miller, *J. Phys. Chem. A*, 1991, **95**, 2881–2888.
15 P. Carcabal, M. Broquier, M. Chevalier, A. Picard-Bersellini, V. Brenner and P. Millié, *J. Chem. Phys.*, 2000, **113**, 4876–4884.
16 Y. Rudich and R. Naaman, *J. Chem. Phys.*, 1992, **96**, 8616–8617.
17 L. Oudejans and R. E. Miller, *J. Phys. Chem. A*, 1999, **103**, 4791–4797.
18 A. J. McCaffery, *Phys. Chem. Chem. Phys.*, 2004, **6**, 1637–1657, and references therein.
19 A. Eppink and D. H. Parker, *Rev. Sci. Instrum.*, 1997, **68**, 3477–3484.
20 D. S. Green and S. C. Wallace, *J. Chem. Phys.*, 1992, **96**, 5857–5877.
21 R. Callaghan, S. Arepalli and R. J. Gordon, *J. Chem. Phys.*, 1987, **86**, 5273–5280.
22 L. Feng, J. Wei and H. Reisler, *J. Phys. Chem. A*, 2004, **108**, 7903–7908.
23 A. H. Nielsen and H. H. Nielsen, *Phys. Rev.*, 1935, **48**, 864–866.
24 V. Dribinski, A. B. Potter, I. Fedorov and H. Reisler, *Chem. Phys. Lett.*, 2004, **385**, 233–238.
25 V. Dribinski, A. B. Potter, I. Fedorov and H. Reisler, *J. Chem. Phys.*, 2004, **121**, 12353–12360.
26 E. Wrede, S. Lanbach, S. Schulenburg, A. Brown, E. R. Wouters, A. J. Orr-Ewing and M. N. R. Ashfold, *J. Chem. Phys.*, 2001, **114**, 2629–2646.
27 B. Chang, R. C. Hoetzlein, J. A. Mudller, J. D. Geiser and P. L. Houston, *Rev. Sci. Instrum.*, 1998, **69**, 1665–1670.
28 V. Dribinski, A. Ossadtchi, V. A. Mandelshtam and H. Reisler, *Rev. Sci. Instrum.*, 2002, **73**, 2634–2642.
29 G. Fischer, R. E. Miller, P. F. Vohralik and R. O. Watts, *J. Chem. Phys.*, 1985, **83**, 1471–1477.
30 M. D. Schuder, C. M. Lovejoy, J. D. D. Nelson and D. J. Nesbitt, *J. Chem. Phys.*, 1989, **91**, 4418–4419.
31 M. D. Schunder, C. M. Lovejoy, R. Lascola and D. J. Nesbitt, *J. Chem. Phys.*, 1993, **99**, 4346–4362.

32 M. Fárník and D. J. Nesbitt, *J. Chem. Phys.*, 2004, **121**, 12386–12395.
33 L. Oudejans, D. T. Moore and R. E. Miller, *J. Chem. Phys.*, 1999, **110**, 209–219.
34 W. H. Press, S. A. Teukolsky, W. T. Vetterling and B. P. Flannery, *Numerical recipes in C*, Cambridge University Press, Cambridge, 1992.
35 J. A. Pople, M. J. Frisch and J. E. Del Bene, *Chem. Phys. Lett.*, 1982, **91**, 185–189.
36 G. B. Bacskay, *Mol. Phys.*, 1992, **77**, 61–73.
37 P. Pechukas and J. C. Light, *J. Chem. Phys.*, 1965, **42**, 3281–3291.
38 M. Zyrianov, A. Sanov, Th. Droz-Georget and H. Reisler, *J. Chem. Phys.*, 1999, **110**, 10774–10783.
39 A. B. Potter, V. Dribinski, A. V. Demyanenko and H. Reisler, *J. Chem. Phys.*, 2003, **119**, 7197–7205.
40 G. E. Ewing, *J. Chem. Phys.*, 1979, **71**, 3143–3144.
41 G. E. Ewing, *J. Phys. Chem.*, 1987, **91**, 4662–4671.
42 J. A. Beswick and J. Jortner, *Adv. Chem. Phys.*, 1981, **47**, 363–506.
43 J. A. Beswick and J. Jortner, *J. Chem. Phys.*, 1980, **74**, 6725–6733.
44 A. J. McCaffery, M. A. Osborne, R. J. Marsh, W. D. Lawrance and E. R. Waclawik, *J. Chem. Phys.*, 2004, **121**, 169–180.
45 R. K. Sampson, S. M. Bellm, A. J. McCaffery and W. D. Lawrance, *J. Chem. Phys.*, 2005, **122**, 74311–74319.
46 S. Bosanac, *Phys. Rev. A*, 1980, **22**, 2617–2622.
47 S. Bosanac and U. Buck, *Chem. Phys. Lett.*, 1981, **81**, 315–319.

